The phagocytosis oxidase/Bem1p domain-containing protein PB1CP negatively regulates the NADPH oxidase RBOHD in plant immunity

Yukihisa Goto[1,2,3] (iD), **Noriko Maki**[1] (iD), **Jan Sklenar**[4] (iD), **Paul Derbyshire**[4] (iD), **Frank L. H. Menke**[4] (iD), **Cyril Zipfel**[3,4] (iD), **Yasuhiro Kadota**[1] (iD) and **Ken Shirasu**[1,2] (iD)

[1]RIKEN Center for Sustainable Resource Science (CSRS), Plant Immunity Research Group, Suehiro-cho 1-7-22 Tsurumi-ku, Yokohama, Kanagawa, 230-0045, Japan; [2]Graduate School of Science, The University of Tokyo, 7-3-1, Hongo, Bunkyo-ku, Tokyo, 113-8654, Japan; [3]Institute of Plant and Microbial Biology, Zurich-Basel Plant Science Center, University of Zurich, Zollikerstrasse 107, Zurich, CH-8008, Switzerland; [4]The Sainsbury Laboratory, University of East Anglia, Norwich Research Park, Norwich, NR4 7UH, UK

Summary

• Perception of pathogen-associated molecular patterns (PAMPs) by surface-localized pattern recognition receptors activates RESPIRATORY BURST OXIDASE HOMOLOG D (RBOHD) through direct phosphorylation by BOTRYTIS-INDUCED KINASE 1 (BIK1) and induces the production of reactive oxygen species (ROS). RBOHD activity must be tightly controlled to avoid the detrimental effects of ROS, but little is known about RBOHD downregulation.

• To understand the regulation of RBOHD, we used co-immunoprecipitation of RBOHD with mass spectrometry analysis and identified PHAGOCYTOSIS OXIDASE/BEM1P (PB1) DOMAIN-CONTAINING PROTEIN (PB1CP).

• PB1CP negatively regulates RBOHD and the resistance against the fungal pathogen *Colletotrichum higginsianum*. PB1CP competes with BIK1 for binding to RBOHD *in vitro*. Furthermore, PAMP treatment enhances the PB1CP-RBOHD interaction, thereby leading to the dissociation of phosphorylated BIK1 from RBOHD *in vivo*. PB1CP localizes at the cell periphery and PAMP treatment induces relocalization of PB1CP and RBOHD to the same small endomembrane compartments. Additionally, overexpression of *PB1CP* in Arabidopsis leads to a reduction in the abundance of RBOHD protein, suggesting the possible involvement of PB1CP in RBOHD endocytosis.

• We found PB1CP, a novel negative regulator of RBOHD, and revealed its possible regulatory mechanisms involving the removal of phosphorylated BIK1 from RBOHD and the promotion of RBOHD endocytosis.

Introduction

The production of reactive oxygen species (ROS) is an immune response against infection that is well-conserved across biological kingdoms. ROS not only possess antimicrobial activities but also function as signaling molecules to trigger additional immune responses (Lambeth *et al.*, 2000). Excessive ROS production can have detrimental effects on cellular functions by damaging DNA, proteins, lipids, and other macromolecules (Moeder & Yoshioka, 2008). As such, ROS production must be produced in the right amount and place, and at the right time to minimize cellular damage.

NADPH oxidases (NOXs) are highly conserved plasma- and endomembrane enzymes that play a crucial role in ROS production in plants, animals, and fungi (Segal, 2016). NADPH oxidases transfer electrons from cytosolic NADPH or NADH to apoplastic oxygen, leading to the production of superoxide (O_2^-), which can then be converted to hydrogen peroxide (H_2O_2) by superoxide dismutases (Marino *et al.*, 2012; Kadota *et al.*, 2015). In animals, the activity of NOX proteins is tightly controlled by regulatory proteins and cytosolic Ca^{2+} levels. The 91-kDa glycoprotein subunit of phagocyte oxidase (GP91[phox]), also known as NADPH oxidase 2 (NOX2), is the best-characterized NOX. NOX2 forms a heterodimer with the membrane protein p22[phox] and together they bind to the cytosolic regulators p47[phox], p67[phox], p40[phox], and the small GTPase Rac. Interaction with these regulators leads to the activation of NOX2 (Canton & Grinstein, 2014). Mutations in NOX2 or its regulatory proteins cause chronic granulomatous disease in which patients suffer from chronic or recurrent bacterial and fungal infections due to the absence of an oxygen burst (Bedard & Krause, 2007), thus showing the crucial role that NOXs play

in immunity. In contrast to NOX2, NOX5 and DUOX have additional EF-hand motifs at the N-terminal domain (ND), suggesting their regulation by Ca^{2+}-binding (Canton & Grinstein, 2014). In addition, Ca^{2+}-dependent kinases, such as protein kinase Cα and Ca^{2+}/calmodulin-dependent protein kinase II, are known to phosphorylate and activate NOX5 and DUOX.

In plants, NOXs belong to the respiratory burst oxidase homolog (RBOH) family, which contains 10 members in *Arabidopsis thaliana* (Torres & Dangl, 2005; Kadota *et al.*, 2015). Among RBOHs, RESPIRATORY BURST OXIDASE HOMOLOG D (RBOHD) plays a particularly crucial role in immunity. *rbohD* knockout mutants are more susceptible to virulent and avirulent strains of the bacterial pathogen *Pseudomonas syringae* (Mersmann *et al.*, 2010; Yuan *et al.*, 2021). Additionally, the double knockout mutant of *rbohD* and its homolog *rbohF* is susceptible to the necrotrophic fungus *Plectosphaerella cucumerina* (Morales *et al.*, 2016). RBOHD homologs are also required for disease resistance against *Botrytis cinerea* in tomato (Li *et al.*, 2015) and *Phytophthora infestans* in *Nicotiana benthamiana* (Asai *et al.*, 2008). Furthermore, RBOHD is also essential for maintaining microbiota homeostasis, as *Xanthomonas* strains that normally colonize wild-type plants without causing symptoms become pathogenic on *rbohD* mutants (Pfeilmeier *et al.*, 2021). In addition, RBOHD-produced ROS are thought to have antimicrobial activities and also play a crucial role in the induction of numerous defense responses, including callose deposition, stomatal closure, and systemic acquired resistance (Mersmann *et al.*, 2010; Luna *et al.*, 2011; Suzuki *et al.*, 2013; Kadota *et al.*, 2015). Furthermore, RBOHD-produced ROS repress the expression of bacterial genes associated with the type II secretion system in opportunistic *Xanthomonas* strains (Yuan *et al.*, 2021; Entila *et al.*, 2023; Pfeilmeier *et al.*, 2023).

Recent studies have clarified the RBOHD activation mechanisms that are triggered after the perception of pathogen-associated molecular patterns (PAMPs) by cell surface-localized pattern recognition receptors (PRRs). Pathogen-associated molecular pattern-induced ROS production by RBOHD is one of the readouts in so-called PRR-triggered immunity (PTI; Kadota *et al.*, 2014; Li *et al.*, 2014). Leucine-rich repeat receptor kinases (LRR-RKs) EFR and FLS2, which are the PRRs for the immunogenic peptides of bacterial EF-Tu and flagellin (elf18 or flg22), respectively, induce instantaneous association with the coreceptor LRR-RLK, BRI1 ASSOCIATED RECEPTOR Kinase 1 (BAK1; Chinchilla *et al.*, 2007; Roux *et al.*, 2011). The PRR complex interacts directly with and phosphorylates receptor-like cytoplasmic kinases (RLCKs) such as BOTRYTIS-INDUCED KINASE 1 (BIK1; Zhang *et al.*, 2010; Liu *et al.*, 2013). The RBOHD forms a complex with EFR and FLS2, and phosphorylated BIK1 interacts directly with, and phosphorylates specific residues at the ND of RBOHD, which is required for RBOHD activation (Kadota *et al.*, 2014; Li *et al.*, 2014). Cysteine-rich RK 2 (CRK2) and MAP4 Kinase SIK1 also contribute to the full activation of RBOD by phosphorylation of specific residues (Zhang *et al.*, 2018; Kimura *et al.*, 2020). In addition to the regulation by BIK1, CRK2, and SIK1, Ca^{2+}-based regulation is also required for RBOHD activation. The PAMP perception by

PRRs activates plasma membrane Ca^{2+} channels such as OSCA1.3 and the cyclic nucleotide-gated channel (CNGC) proteins CNGC2 and CNGC4 (at least under specific Ca^{2+} concentrations) through BIK1, which lead to the influx of Ca^{2+} (Tian *et al.*, 2019; Thor *et al.*, 2020). Ca^{2+}, in turn, activates RBOHD through Ca^{2+} binding to the EF-hand motif in RBOHD-ND as well as through phosphorylation by Ca^{2+}-dependent protein kinases (CPKs; Kobayashi *et al.*, 2007; Ogasawara *et al.*, 2008; Dubiella *et al.*, 2013). Small GTPase RAC also binds to the ND of the RBOHD homolog in rice and is involved in the activation (Wong *et al.*, 2007).

The RBOHD is also activated upon recognition of pathogen effectors by intracellular immune receptors known as nucleotide-binding leucine-rich repeat (NLR) receptors, leading to NLR-triggered immunity (NTI). Similar to the RBOHD activation during PTI, the involvement of CPKs and BIK1 has also been demonstrated in the activation of RBOHD during NTI (Gao *et al.*, 2013; Yuan *et al.*, 2021), suggesting common activation mechanism of RBOHD. In contrast to the well-characterized mechanisms of RBOHD activation, the processes involved in downregulation of RBOHD are not well understood. Nitric oxide production may be involved in the downregulation of RBOHD by s-nitrosylation on the C-terminus residue required for FAD binding (Yun *et al.*, 2011). However, it is still unknown whether similar mechanisms also occur during PTI. A recent study showed that translation initiation factor binding protein CBE1 and certain translation factors negatively regulate the accumulation of RBOHD, but their roles in halting ROS production are unknown (George *et al.*, 2023). Endocytosis and vacuolar degradation are potential mechanisms involved in the downregulation of RBOHD, as these processes are known to decrease membrane proteins and their activity in the downstream signaling pathways. For example, many PRRs are endocytosed after ligand perception through the clathrin-mediated pathway (Robatzek *et al.*, 2006; Mbengue *et al.*, 2016). Interestingly, PBS1-LIKE KINASES (PBL13), an RLCK, phosphorylates the C-terminal domain (CD) of RBOHD, which triggers the ubiquitination of RBOHD by PIRE (PBL13-INTERACTING RING DOMAIN E3 LIGASE; Lin *et al.*, 2015; Lee *et al.*, 2020). Because PIRE-mediated ubiquitination of RBOHD lowers the protein levels, ubiquitination may serve as a signal for endocytosis and vacuolar degradation. However, the precise mechanism by which PAMP-induced ROS production is terminated remains elusive, particularly regarding whether endocytosis or vacuolar degradation of RBOHD is induced as a mean to halt ROS production. It is also noteworthy that, although RBOHs and animal NOX2 are structurally similar, apart from RAC, all the known regulators of RBOHD are plant-specific components. Notably, none of the known regulators of NOX2 in animals have been found to have a regulatory role in the context of RBOHs in plants.

In this work, we aimed to investigate the regulatory mechanism of RBOHD during PTI to elucidate how plants effectively utilize ROS to combat pathogens and activate signaling pathways, while minimizing the potential toxic effects. We identified phagocytosis oxidase/Bem1p (PB1) domain-containing protein (PB1CP) as a novel component of RBOHD complex. Through

functional analyses of knockout mutants and overexpression lines, we demonstrated that PB1CP acts as a negative regulator of RBOHD activity and is involved in RBOHD-mediated fungal immunity. Furthermore, our biochemical and microscopic analyses provided insights into the potential regulatory mechanisms of RBOHD by PB1CP through the removal of phosphorylated BIK1 from RBOHD and the promotion of RBOHD endocytosis. These findings contribute to a better understanding of the downregulation of RBOHD which possibly contributes to fine-tuning their ROS production and maintaining a balanced immune response.

Materials and Methods

Plant materials and growth conditions

Arabidopsis thaliana (L.) Heynh plants were grown on soil under an 8 or 16 h photoperiod at 23°C, or in a half-strength MS medium containing 1% sucrose under a continuous light photoperiod at 23°C. *Nicotiana benthamiana* plants were soil-grown under a 16 h photoperiod at 22°C.

Transgenic lines and T-DNA insertion lines

Arabidopsis stable transgenic lines of *p35S:PB1CP-3xHA* (epiGreenB5) were generated by the floral drop and floral dip methods. T-DNA insertion mutant lines, *pb1cp-1* (SALK_036544) and *pb1cp-2* (SALK_207053) were obtained from the Arabidopsis Biological Resource Center at the Ohio State University. Previously published lines were as follows: *rbohD* (Torres *et al.*, 2002), *rbohD/pRBOHD:3xFLAG-gRBOHD* and *rbohD/pRBOHD:3xFLAG-gRBOHD-S343A/S347A* (Kadota *et al.*, 2014).

Protein extraction and co-immunoprecipitation

Protein extraction and immunoprecipitation were performed as described previously (Kadota *et al.*, 2014, 2016) with minor modifications. For large-scale immunoprecipitation to identify RBOHD-associated proteins, 10 g of fresh-weight Arabidopsis seedlings were used. The seedlings were ground with sand (Sigma-Aldrich) in liquid nitrogen, and an extraction buffer consisting of 50 mM Tris–HCl (pH 7.5), 150 mM NaCl, 10% glycerol, 5 mM DTT, 2.5 mM NaF, 1 mM $Na_2MoO_4 \cdot 2H_2O$, 0.5% (w/v) polyvinylpyrrolidone, 1% (v/v) P9599 Protease Inhibitor Cocktail (Sigma-Aldrich), 100 μM phenylmethylsulphonyl fluoride, 2% (v/v) IGEPAL CA-630 (Sigma-Aldrich), 2 mM EDTA, and 1% (v/v) protein phosphatase inhibitor cocktail 2 and 3 (Sigma-Aldrich) was added at a concentration of 2 ml g^{-1} tissue powder. The samples were incubated at 4°C for 1 h and clarified through multiple centrifugations at 16 000 g for 20 min at 4°C. Supernatant protein concentrations were adjusted to 5 mg ml^{-1} and then incubated for 2 h at 4°C with 200 μl of α-FLAG matrix (Sigma-Aldrich) for co-immunoprecipitation with 3xFLAG-RBOHD. Subsequently, the matrix was subjected to three washes with the extraction buffer, and 3xFLAG peptides were employed to elute 3xFLAG-RBOHD, thereby eliminating the elution of any nonspecific interactors to the beads. For small-scale co-immunoprecipitations with PB1CP-HA, we used 2 g of Arabidopsis seedlings of *p35S:PB1CP-3xHA* line, while for co-immunoprecipitation with 3xFLAG-RBOHD transiently expressed in *N. benthamiana*, we used four leaves harvested 3 d after Agroinfiltration. In these experiments, we followed the same protocol, except 1% (v/v) IGEPAL CA-630 was included in the extraction buffer, and α-HA magnetic beads and α-FLAG magnetic beads (Miltenyi Biotec, Bergisch Gladbach, Germany) were used for capturing the proteins and boiled SDS sample buffer was used for the elution.

ROS burst assay

Eight or 16 leaf disks (4 mm in diameter) were collected from 4- to 6-wk-old Arabidopsis plants or 5-wk-old *N. benthamiana*. The leaf disks were then floated overnight on sterile water. The next day, the water was replaced with a solution containing 40 μM Luminol (FUJIFILM Wako Pure Chemical Corporation, Osaka, Japan), 20 μg ml^{-1} horseradish peroxidase (HRP; Sigma-Aldrich), and 1 μM flg22 or 1 μM elf18 for the detection of flg22- or elf18-induced ROS production. For the detection of chitin-induced ROS production, a solution containing 1 μM L-012 (FUJIFILM Wako Pure Chemical Corporation), 20 μg ml^{-1} HRP, and 10 μM chitin ((GlcNAc)$_7$) was used. Luminescence was measured using a Tristar2 multimode reader (Berthold Technologies, Baden-Wurttemberg, Germany) or a TECAN Spark microplate reader (Tecan, Männedorf, Switzerland).

Confocal microscopy analyses

Four-week-old *N. benthamiana* leaves were used to observe the subcellular localization of PB1CP-GFP and CFP-RBOHD. The fluorescence signals of GFP, CFP, and FM4-64 were recorded using confocal laser scanning microscopy (Leica TCS SP5; Leica Microsystems GmbH, Wetzlar Germany) after excitation at 488 nm for GFP and FM4-64 or 433 nm for CFP with an argon laser. The micrographs were processed using LAS X v.3.3.0.16799 and FIJI software (Schindelin *et al.*, 2012).

Other methods

Protein identification by LC–MS/MS, vector construction, transient expression in *N. benthamiana*, MAPK activation assay, immunoblotting, *C. higginsianum* infection assay, bacterial infection assays, RT-qPCR assay, phylogenetic analyses, *in vitro* pulldown assay, and statistical analyses were performed as described previously (Narusaka *et al.*, 2010; Kadota *et al.*, 2014, 2016; Hiruma & Saijo, 2016; Goto *et al.*, 2020) with minor modifications detailed in Supporting Information Methods S1.

Results

PB1CP is a novel interactor of RBOHD during PTI

To understand the regulatory mechanism of PAMP-induced ROS production during PTI, we employed co-immunoprecipitation

coupled with liquid chromatography–tandem mass spectrometry (LC–MS/MS) to identify novel regulators of RBOHD in Arabidopsis. We used a stable transgenic Arabidopsis line expressing 3xFLAG-tagged RBOHD under the control of its native promoter in *rbohD* knockout background (*rbohD*/*pRBOHD:3xFLAG-gRBOHD*; Kadota *et al.*, 2014). Plants were treated with elf18 or with elf18 and flg22 simultaneously (elf18 + flg22) to activate RBOHD. 3xFLAG-RBOHD was immunoprecipitated using α-FLAG antibody and eluted by competition with 3xFLAG peptide, and RBOHD-associated proteins were identified by LC–MS/MS (Fig. S1a; Table S1). In three independent experiments, we identified 450 candidate RBOHD-associated proteins. Among those candidates, there were proteins known to associate with RBOHD, such as CRK2 (Kimura *et al.*, 2020) and extra-large guanine nucleotide-binding protein 3 (XLG3; Liang *et al.*, 2016). There were also known PRR interactors such as BAK1 (Chinchilla *et al.*, 2007), CERK1 (Miya *et al.*, 2007), FER (Stegmann *et al.*, 2017), IOS1 (Yeh *et al.*, 2016), the cyclic nucleotide-gated ion channels CNGC2 and CNGC4 (Tian *et al.*, 2019), as well as the plasma membrane Ca^{2+}-ATPases ACA8 and ACA10 (Frei Dit Frey *et al.*, 2012; Table S1). These proteins were not unexpected as we had previously shown that RBOHD associates with EFR and FLS2 even before PAMP recognition (Kadota *et al.*, 2014). Consistent with the observation that BAK1 interacts with EFR and FLS2 in a ligand-dependent manner (Chinchilla *et al.*, 2007; Roux *et al.*, 2011; Sun *et al.*, 2013), a higher amount of BAK1 was co-eluted with RBOHD after PAMP treatment (Fig. S1b; Table S1). These results show that the methods employed are effective for isolating active PRR–RBOHD complex(es) containing BAK1. However, it is important to consider the presence of possible false-positive candidates that may reside in close proximity to RBOHD at the plasma membrane but do not directly interact with it. This is particularly relevant due to the unique structure of RBOHD, which possesses six membrane-spanning domains. Undigested membranes that are associated with RBOHD might co-elute together, even in the presence of a detergent such as 2% IGEPAL CA-630, leading to the contamination of membrane proteins within the undigested membranes. This could potentially account for the larger number of candidate RBOHD-associated proteins than initially expected.

To narrow down the candidates, we selected 30 candidate proteins based on the strength of their interaction with RBOHD and their potential functional involvement in the activation of RBOHD by PAMPs. The candidate genes were expressed under the control of the cauliflower mosaic virus (CaMV) 35S promoter (p35S) in *N. benthamiana* and ROS production was measured after induction with flg22 (Fig. S2; Table S2a). The effect of each candidate protein on flg22-induced ROS production was evaluated by comparing the regions where candidate proteins or GUS proteins (as negative control) were expressed in the same leaves under the control of the CaMV 35S promoter. As a positive control, we expressed BIK1 and checked the effect on flg22-induced ROS production. As expected, BIK1 expression resulted in a significant increase in flg22-induced ROS production (Fig. S2). Among 30 candidates, six genes significantly suppressed flg22-induced ROS

production, and none increased it (Table S2a). The six candidate negative regulators are KARYOPHERIN ENABLING THE TRANSPORT OF THE CYTOPLASMIC HYL1 (AT5G19820), 2-oxoglutarate dehydrogenase E1 component (AT3G55410), lipase/lipoxygenase plat domain protein 2 (AT2G22170), an LRR-RK (AT3G02880), N-TERMINAL-TRANSMEMBRANE C2 DOMAIN PROTEINS TYPE 4/Ca^{2+}-DEPENDENT LIPID-BINDING PROTEIN 1/SYNAPTOTAGMIN 7 (AT3G61050), and PB1CP (AT2G01190). PB1CP is the focus of the present study because a PB1 domain is conserved in p40^{phox} and p67^{phox}, which are important regulators of NOX2 in animals, while other candidates will be described elsewhere. The PB1 domain functions as a protein-binding module through *PB1*-mediated heterodimerization or homo-oligomerization. For example, the p40^{phox} and p67^{phox} proteins interact with each other through their PB1 domains, which facilitate the assembly of NOX2 and the cytosolic regulators p22^{phox}, p40^{phox}, and Rac at the membrane (Groemping & Rittinger, 2005; Sumimoto, 2008). Such assembly results in NOX2-mediated production of O_2^- (Canton & Grinstein, 2014). Co-immunoprecipitation with 3xFLAG-RBOHD indicated a total of three unique peptides corresponding to PB1CP from untreated, elf18, and elf18 + flg22-treated samples (Fig. S1; Table 1). The expression of *PB1CP* under the control of the CaMV 35S or native promoters significantly reduced flg22-induced ROS production in *N. benthamiana* (Figs 1, S3). These results suggest that PB1CP negatively regulates flg22-induced ROS production. This contrasts with p40^{phox} and p67^{phox}, which positively regulate NOX2.

## PB1CP negatively regulates PAMPs-induced ROS production in Arabidopsis

PB1 domains range from 80 to 100 amino acids in length and exhibit a ubiquitin-like β-grasp fold with five β-sheets and two α-helices (Müller *et al.*, 2006). Arabidopsis encodes > 80 PB1 domain-containing proteins, which can be classified into eight families based on domain architecture (Mutte & Weijers, 2020). PB1CP belongs to the plant-specific 'kinase-derived family', which is characterized by a single PB1 domain in the ND with a large flanking sequence devoid of known domains. The PB1 domains of 'kinase-derived family' members share similarities with those of the 'kinase domain family' (Fig. S4). It is likely that kinase-derived family might have evolved from the kinase domain family in the ancestors of angiosperms (Mutte & Weijers, 2020).

To clarify the role of PB1CP during PTI, we characterized two independent *pb1cp* mutants, *pb1cp-1* (SALK_036544) and *pb1cp-2* (SALK_207053). The *pb1cp-2* allele has a T-DNA insertion at the second exon, resulting in a potentially null mutant (Fig. S5a). By contrast, the *pb1cp-1* allele is unlikely null as it has T-DNA insertion within the 5′ UTR that results in a significant reduction in *PB1CP* transcript levels (Fig. S5b). These *pb1cp* mutants did not show any obvious phenotypic abnormalities (Fig. S5c). Upon treatment with flg22 or elf18, Col-0 plants induced biphasic production of ROS, while chitin treatment resulted in transient ROS production. By contrast, *pb1cp-2 mutant* significantly enhanced biphasic ROS

Table 1 Peptide counts of PB1CP in 3xFLAG-RBOHD Co-IP analysis.

PB1CP peptides identification by co-immunoprecipitation of 3xFLAG-RBOHD and LC–MS/MS Analysis				
Treatment	Peptide sequence	Probability (%)	Best mascot score	Number of spectra
Mock	(K)SDDWFLNALNSAGLLNR(G)	100	51.56	3
elf18	(K)SDDWFLNALNSAGLLNR(G)	100	40.03	2
elf18 + flg22	(K)SDDWFLNALNSAGLLNR(G)	100	32.69	1
	(R)LLGLDDALALR(S)	99	35.49	2
	(R)VHVEEPGGVR(T)	96	20.71	1

Fig. 1 Heterologous expression of PB1CP-GFP under the native Arabidopsis promoter reduces flg22-induced reactive oxygen species (ROS) production in *Nicotiana benthamiana*. (a, b) PB1CP-GFP (*pPB1CP:gPB1CP-GFP*) and free GFP (*p35S:GFP*) were expressed in the same leaf by Agroinfiltration, and flg22-induced ROS was measured by a luminol-based assay after 3 d post-inoculation (dpi). Time-course (a) and the total amount (b) of ROS production induced by 1 μM flg22. Values are mean ± standard error (SE; $n = 8$). Asterisks indicate a significant difference based on Student's t-test (**, $P \leq 0.01$). (c) The protein expression of PB1CP-GFP was confirmed by immunoblot analysis with α-GFP antibody. The experiments were repeated three times with similar results.
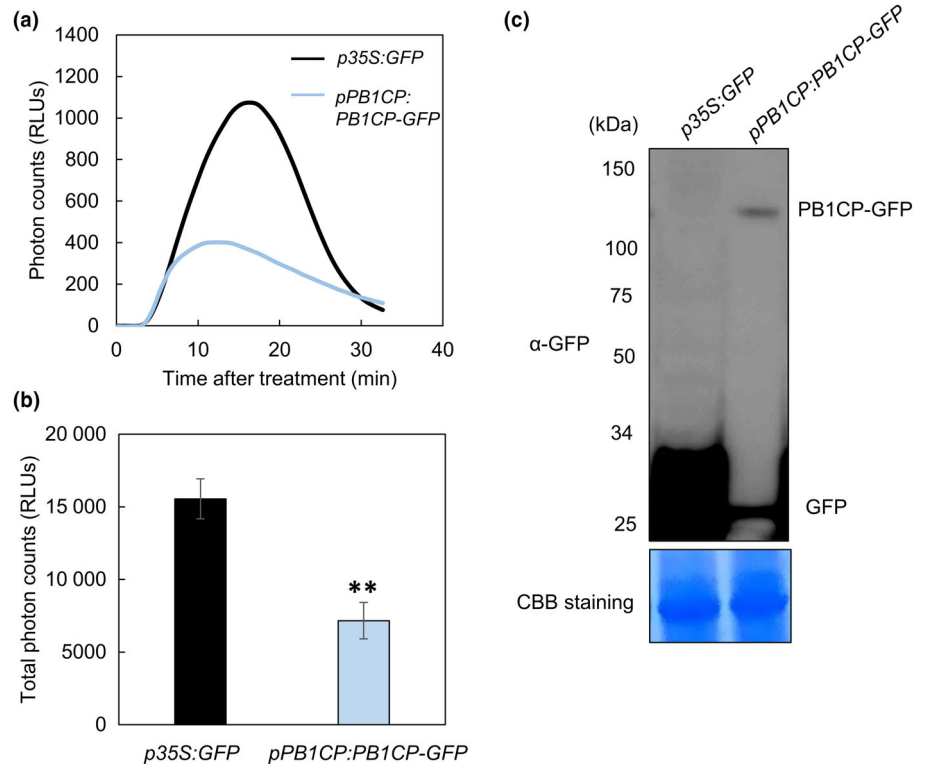
production upon flg22 or elf18 treatment and enhanced the transient ROS production following chitin treatment compared with Col-0 (Fig. 2a–c). Although the *pb1cp-1* mutant showed a relatively milder phenotype, it still exhibited a significant enhancement in flg22-inducible biphasic ROS production, as well as the first peak of elf18-induced ROS production and chitin-induced ROS production. In contrast to the enhanced ROS production, the *pb1cp* mutants did not show any difference in flg22-induced MAPK activation (Fig. 2d), which is a ROS-independent signaling event during PTI (Shinya *et al.*, 2014). These results suggest that PB1CP is specifically involved in ROS production.

To further investigate the role of PB1CP during PTI, we generated two independent Arabidopsis transgenic lines overexpressing PB1CP-3xHA under the control of the CaMV 35S promoter (*p35S:PB1CP-3xHA*; Fig. S6). These lines express three to four times higher *PB1CP* compared with Col-0 (Fig. S6b). Similar to the *pb1cp* mutants, neither *p35S:PB1CP-3xHA* line differed phenotypically from the wild-type (Fig. S6c). In contrast to the *pb1cp* mutants, *p35S:PB1CP-3xHA* lines induced significantly

less ROS production upon treatment with flg22, elf18, or chitin, compared with Col-0 (Fig. 3a–c), while flg22-induced MAPK activation was unchanged in the transgenic lines (Fig. 3d). Based on these results, we concluded that PB1CP plays a specific negative regulatory role in RBOHD-mediated ROS production in Arabidopsis.

We observed a transcriptional upregulation of PB1CP during PTI, specifically in response to treatment with elf18 and chitin, but not flg22. The treatment with elf18 or chitin led to a slight increase in the accumulation of PB1CP transcript levels (Fig. S7). We also checked the role of PB1CP on the expression of *RBOHD* by using *pb1cp-2* and *p35S:PB1CP-3xHA* lines, but there is no effect of PB1CP on *RBOHD* expression (Fig. S8).

PB1CP negatively regulates the resistance against *C. higginsianum*

To test whether there is a link between PB1CP-mediated regulation of ROS production and disease resistance, we measured resistance against the weakly virulent bacterial strain *Pseudomonas*
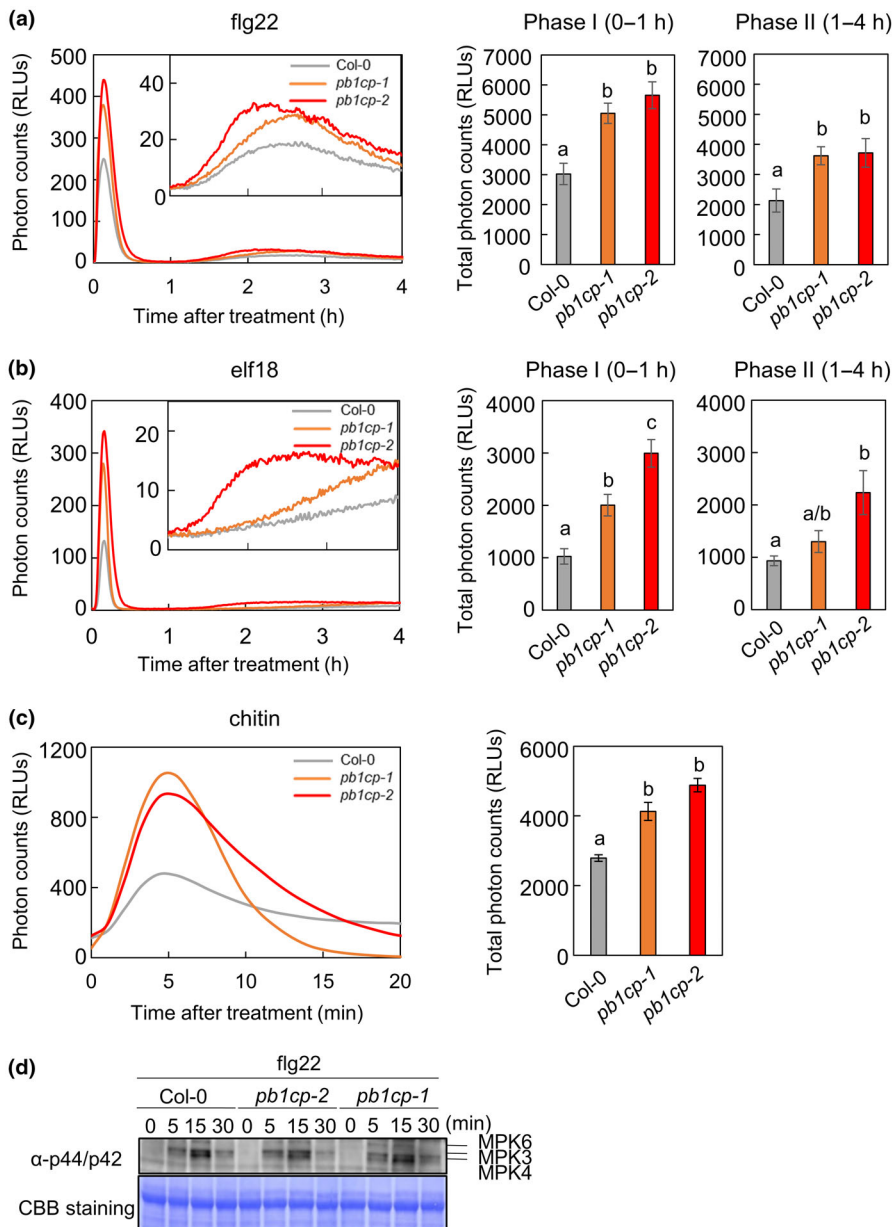
Fig. 2 *pb1cp* mutants have higher pathogen-associated molecular pattern (PAMP)-induced reactive oxygen species (ROS) production but normal MAPK activation. Time-course of ROS production was monitored upon treatment with 1 µM flg22 (a), 1 µM elf18 (b), and 10 µM chitin ((GlcNAc)$_7$) (c) in *pb1cp* mutants. In addition, the total amount of ROS production induced by flg22 or elf18 during phase I (0–1 h) and phase II (1–4 h), as well as the total amount of chitin-induced ROS production, were quantified. Sixteen leaf disks from eight 5-wk-old Arabidopsis plants were used for ROS assays. Values are mean ± SE (*n* = 16). Different characters indicate significant differences based on one-way ANOVA and Tukey's *post hoc* test (*P* ≤ 0.05). (d) flg22-Induced activation of MAPKs in *pb1cp* mutants. Ten-day-old Arabidopsis seedlings were treated with 1 µM flg22 and phosphorylated MAPKs were detected on immunoblots with α-phospho-p44/42 MAPK (Erk1/2; Thr202/Tyr204) antibody. Equal loading of protein samples is shown by CBB staining. All the experiments were repeated three times with similar results.

syringae pv *tomato* (*Pto*) DC3000 *COR⁻* that lacks the toxin coronatine (COR) to trigger stomatal reopening during infection (Melotto *et al.*, 2008), and the nonadapted bacterium *Pseudomonas syringae* pv *cilantro* (*Pci*) 0788-9, which grows very poorly on Col-0 plants (Lewis *et al.*, 2008). Six-week-old Arabidopsis plants were spray-inoculated with *Pto* DC3000 *COR⁻* and *Pci* 0788-9. There was no difference in bacterial growth of *Pto* DC3000 *COR⁻* and *Pci* 0788-9 in the *pb1cp* mutants or *p35S:PB1CP-3xHA* lines, compared with Col-0 (Fig. S9). This indicates that the altered levels of ROS by PB1CP may not have a substantial impact on PAMP-induced stomatal closure (Melotto *et al.*, 2008). However, we found RBOHD plays an important role in the resistance against the fungal pathogen *C. higginsianum* and PB1CP negatively regulates the resistance. Four-week-old

Arabidopsis leaves were drop-inoculated with *C. higginsianum* and lesion diameters were measured. Lesion diameters were found to be increased in *rbohD* mutants. S343 in ND of RBOHD is a critical phosphorylation site targeted by BIK1 and S347 is targeted by BIK1 and CPKs for the activation of RBOHD during PTI and NTI (Dubiella *et al.*, 2013; Kadota *et al.*, 2014, 2019; Li *et al.*, 2014). The lesion diameters were also increased in the transgenic plants carrying mutations in RBOHD at the phosphorylation sites (*rbohD/pRBOHD:3xFLAG-gRBOHD* S343A/S347A), showing crucial roles of RBOHD and its phosphorylation sites in the resistance against *C. higginsianum* (Fig. 4a). Importantly, lesion diameters were smaller in the *pb1cp* mutants (Fig. 4b) and larger in *p35S:PB1CP-3xHA* lines than Col-0 (Fig. 4c). We also assessed the biomass of *C. higginsianum*
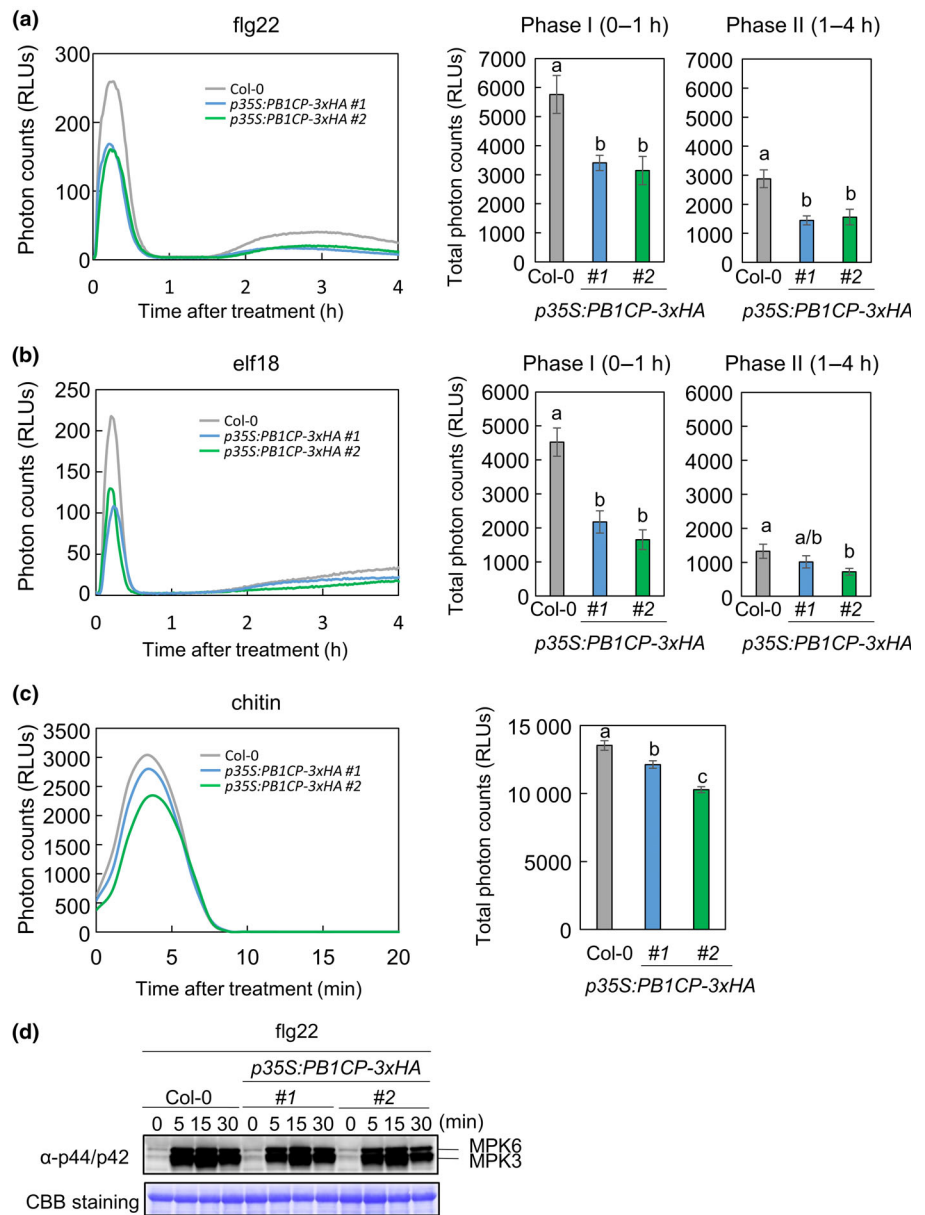
Fig. 3 *p35S:PB1CP-3xHA* lines have reduced pathogen-associated molecular pattern (PAMP)-induced reactive oxygen species (ROS) production but normal MAPK activation. Time-course of ROS production was monitored upon treatment with 1 μM flg22 (a), 1 μM elf18 (b), and 10 μM chitin ($(GlcNAc)_7$) (c) in *PB1CP* overexpression lines (*p35S:PB1CP-3xHA*#1 and #2). In addition, the total amount of ROS production induced by flg22 or elf18 during phase I (0–1 h) and phase II (1–4 h), as well as the total amount of chitin-induced ROS production, were quantified. Sixteen leaf disks from eight 5-wk-old Arabidopsis plants were used for ROS assays. Values are mean ± SE ($n = 16$). Different characters indicate significant differences based on one-way ANOVA and Tukey's *post hoc* test ($P \leq 0.05$). (d) flg22-Induced activation of MAPKs in *p35S:PB1CP-3xHA* lines. Ten-day-old Arabidopsis seedlings were treated with 1 μM flg22, and phosphorylated MAPKs were detected on immunoblots with α-phospho-p44/42 MAPK (Erk1/2; Thr202/Tyr204) antibody. Equal loading of protein samples is shown by CBB staining. All the experiments were repeated three times with similar results.

by quantification of actin (*ChACT*) mRNA using RT-qPCR (Narusaka *et al.*, 2010; Fig. 4d). Although we did not observe a statistically significant decrease in *C. higginsianum* growth in the *pb1cp-2* mutant compared with Col-0, we did observe enhanced growth of *C. higginsianum* in the *p35S:PB1CP-3xHA* line and *rbohD* mutant, compared with Col-0. These results suggest that PB1CP negatively regulates resistance against *C. higginsianum*. Considering that *C. higginsianum* relies on penetrating the plant cell wall and invaginating into the cell by manipulating the host plasma membrane during infection (O'Connell *et al.*, 2012), it is reasonable to speculate that the fungus may be more susceptible to ROS than bacterial pathogens due to its close interaction with the plasma membrane during these processes. The proximity to the plasma membrane increases the likelihood of ROS exposure, which can have detrimental effects on the fungus's viability and survival.

Flg22-induced interaction of PB1CP with RBOHD results in the release of phosphorylated BIK1

To confirm PB1CP-RBOHD interaction, we performed immunoprecipitation of PB1CP-3xHA with α-HA antibody from the *PB1CP-3xHA* (*p35S:PB1CP-3xHA*) Arabidopsis line to see the interaction of PB1CP-3xHA with endogenous RBOHD by α-RBOHD antibody. PB1CP associated weakly with endogenous RBOHD (Fig. 5a). However, the treatment with elf18 or flg22 for 10 min increased PB1CP-RBOHD association. There was a similar but weaker effect of elf18, perhaps due to the absence of EFR protein in Arabidopsis roots (Wu *et al.*, 2016).

An *in vitro* binding assay using recombinant proteins was used to test whether PB1CP and RBOHD bind directly (Fig. 5b). Although we were unable to obtain full-length PB1CP recombinant protein, we were able to express domains of PB1CP (ND,
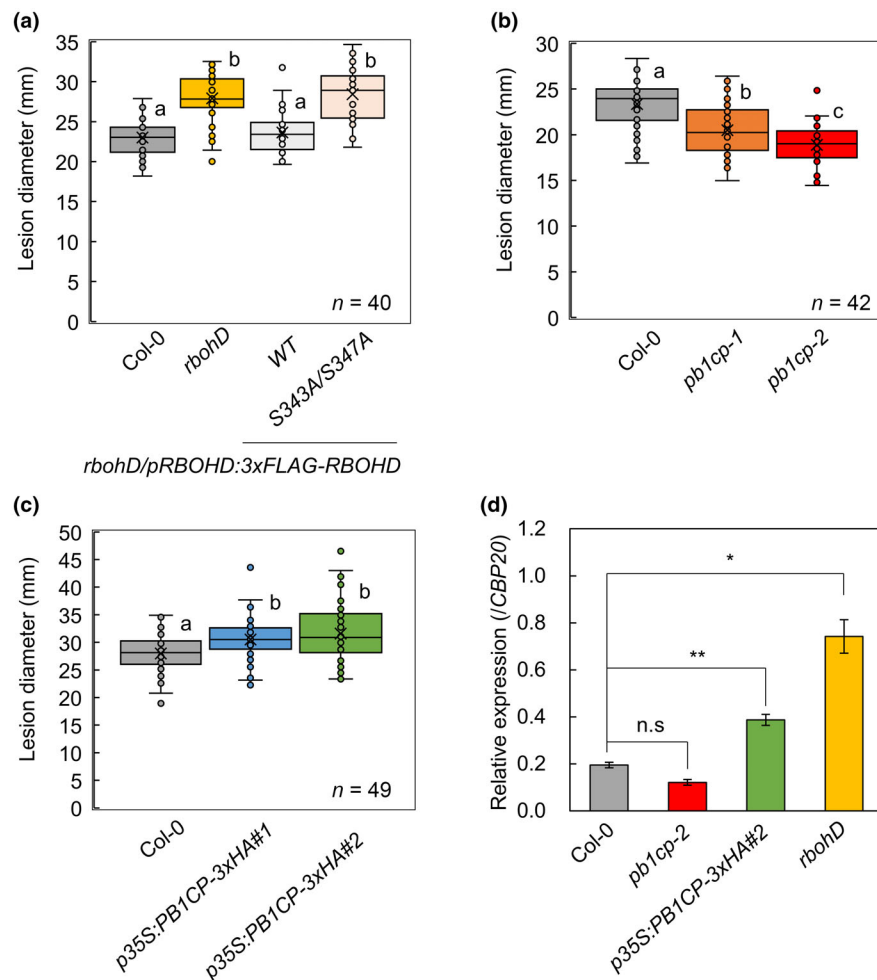
Fig. 4 Resistance against *Colletotrichum higginsianum* is dependent on RESPIRATORY BURST OXIDASE HOMOLOG D (RBOHD) and its phosphorylation sites, while PB1CP negatively regulates the resistance. The diameters of necrotic lesions resulting from *C. higginsianum* infection were measured in different genotypes: *rbohD* mutants, *rbohD/pRBOHD:3xFLAG-RBOHD* (WT) line, the phosphorylation site mutants (*S343A/S347A*) (a), *pb1cp* mutants (b), and *p35S:PB1CP-3xHA#1 and #2* lines (c). Four-week-old Arabidopsis plants grown in soil were drop-inoculated with *C. higginsianum* to induce lesion formation. In each box plot, the central horizontal line indicates the median value, the black cross indicates the mean value, the lower box limit shows the value of the first quartile, the upper box limit depicts the third quartile, the whiskers indicate values within the 1.5-fold interquartile range, and each open circle represents one sample data point. The numbers of necrotic lesions measured were indicated in the graphs. Different characters indicate significant differences based on one-way ANOVA and Tukey's *post hoc* test ($P \leq 0.05$). We conducted the statistical analyses twice: once including all data points and once excluding outliers (sample data points outside the range of the whiskers in the box plots). In both scenarios, the results remained consistent. The experiments were repeated three times with similar results. The quantification of *C. higginsianum* in different genotypes: *rbohd*, *pb1cp-2*, and *p35S:PB1CP-3xHA#2* line (d). Four-week-old plants were spray-inoculated with *C. higginsianum*, and at 4 d post-inoculation (dpi), the inoculated leaves were harvested for total RNA isolation. RT-qPCR was performed to quantify *ChACT* over *AtCBP20* transcript levels. Values are mean $\pm$ SE of four biological replicates. Asterisks indicate significant differences compared with the values indicated by the lines (Student's *t*-test; *, $P \leq 0.05$; **, $P \leq 0.01$).

PB1 domain (PB1D), and CD) in *E. coli*. *In vitro* pull-down assays showed that Maltose-Binding Protein (MBP)-tagged PB1CP-CD (MBP- PB1CP-CD), but not MBP-PB1CP-ND nor MBP-PB1D, bind directly with glutathione S-transferase (GST)-tagged RBOHD-ND (GST-RBOHD-ND). Furthermore, MBP-PB1CP-CD competed with MBP-BIK1 for GST-RBOHD-ND binding (Fig. 5c), suggesting that PB1CP-CD and BIK1 share an overlapping binding region of RBOHD-ND. To validate the *in vivo* competition, we expressed FLAG-RBOHD and BIK1-HA with or without PB1CP-GFP in *N. benthamiana* and monitored the RBOHD-BIK1 interaction by co-immunoprecipitation assay (Fig. 5d). We observed that RBOHD

formed a *constitutive* association with nonphosphorylated BIK1. The treatment with flg22 induced a mobility shift in BIK1, which is attributed to its phosphorylation and activation by BAK1 (Lu *et al.*, 2010; Zhang *et al.*, 2010). Furthermore, we found that phosphorylated BIK1 (upper band) co-immunoprecipitated with FLAG-RBOHD, confirming the formation of a complex between RBOHD and phosphorylated BIK1 as shown previously (Kadota *et al.*, 2014). While PB1CP exhibited a weak association with RBOHD, the interaction was enhanced by flg22 treatment. Importantly, the flg22-induced interaction between PB1CP and RBOHD resulted in a reduction in the interaction between RBOHD and phosphorylated BIK1,
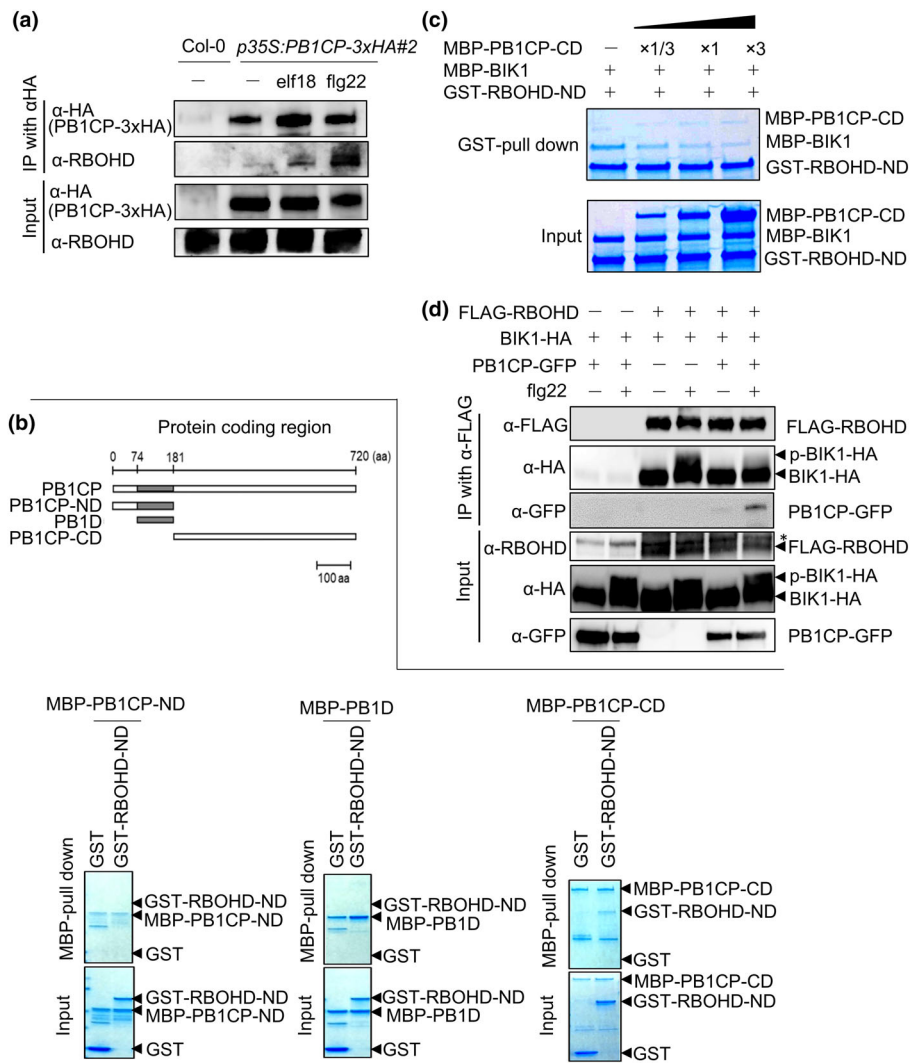
Fig. 5 Pathogen-associated molecular pattern (PAMP) treatment enhances the direct interaction between PB1CP and RESPIRATORY BURST OXIDASE HOMOLOG D (RBOHD), thereby reducing the interaction between RBOHD and phosphorylated BOTRYTIS-INDUCED KINASE (BIK1). (a) The treatment with elf18 or flg22 enhances PB1CP-RBOHD binding in Arabidopsis. Stable transgenic Arabidopsis seedlings of *p35S:PB1CP-3xHA* or Col-0 were treated with or without 1 μM flg22 or 1 μM elf18 for 10 min. Untreated plants (−) served as controls. Total proteins (input) were immunoprecipitated with α-HA magnetic beads followed by immunoblots with α-HA and α-RBOHD antibodies. Wild-type Col-0 served as a negative control to demonstrate the absence of any nonspecific interaction of RBOHD to the beads. (b) PB1CP-C-terminal domain (PB1CP-CD) directly interacts with RBOHD-N-terminal domain (RBOHD-ND) *in vitro*. MBP-PB1CP-ND, MBP-PB1D (PB1 domain), or MBP-PB1CP-CD were incubated with GST-RBOHD-ND or GST and pulled down with MBP. Input and pull-down proteins were separated by SDS-PAGE and stained with CBB. (c) PB1CP competes with BIK1 for binding to RBOHD. MBP-BIK1 was incubated with GST-RBOHD-ND with increasing amounts of MBP-PB1CP-CD, and pulled down with GST. All experiments were performed more than three times with similar results. (d) Flg22-induced PB1CP interaction with RBOHD led to a reduction in the interaction between RBOHD and phosphorylated BIK1 in *Nicotiana benthamiana*. FLAG-RBOHD and BIK1-HA were transiently expressed with or without PB1CP-GFP in *N. benthamiana* leaves and were treated with or without 1 μM flg22 for 10 min. Total proteins (input) were immunoprecipitated with α-FLAG magnetic beads followed by immunoblots with α-FLAG, α-HA, and α-GFP antibodies. The samples without expression of FLAG-RBOHD served as a negative control to demonstrate the absence of any nonspecific interaction of BIK1-HA and PB1CP-GFP to the beads. α-RBOHD antibody was used to detect FLAG-RBOHD only in the input because very strong nonspecific bands of the same size as FLAG-RBOHD were observed even in the absence of its expression. Nonspecific bands are denoted with an asterisk. All the experiments were repeated three times with similar results.

highlighting the competitive relationship between PB1CP and BIK1 in the activation of RBOHD.

PAMP treatment induces PB1CP accumulation in endomembrane compartments

To understand further how PB1CP regulates RBOHD, we monitored its subcellular localization by transiently expressing

PB1CP-GFP in leaves of *N. benthamiana* by Agroinfiltration under the control of its native promoter (*pPB1CP: gPB1CP-GFP*). Confocal microscopy analyses showed that the PB1CP-GFP signal predominantly localized at the cell periphery, exhibiting co-localization with the plasma membrane as visualized by FM4-64 staining (Fig. 6a). We also observed that small PB1CP-GFP signal foci moved around the cell periphery and within the cytoplasm (Video S1). Interestingly, the

treatment with flg22 or chitin for 3–6 h reduced PB1CP-GFP signals in the cell periphery, accompanied by the emergence of numerous PB1CP-GFP signal foci in the cell periphery and within the cytoplasm (Fig. 6b; Video S2). Notably, the PB1CP-GFP foci that appeared following flg22 treatment exhibited clear co-localization with FM4-64 dye, an endocytic tracer, indicating their localization within small endomembrane compartments (Fig. 6c). These results suggest that PB1CP
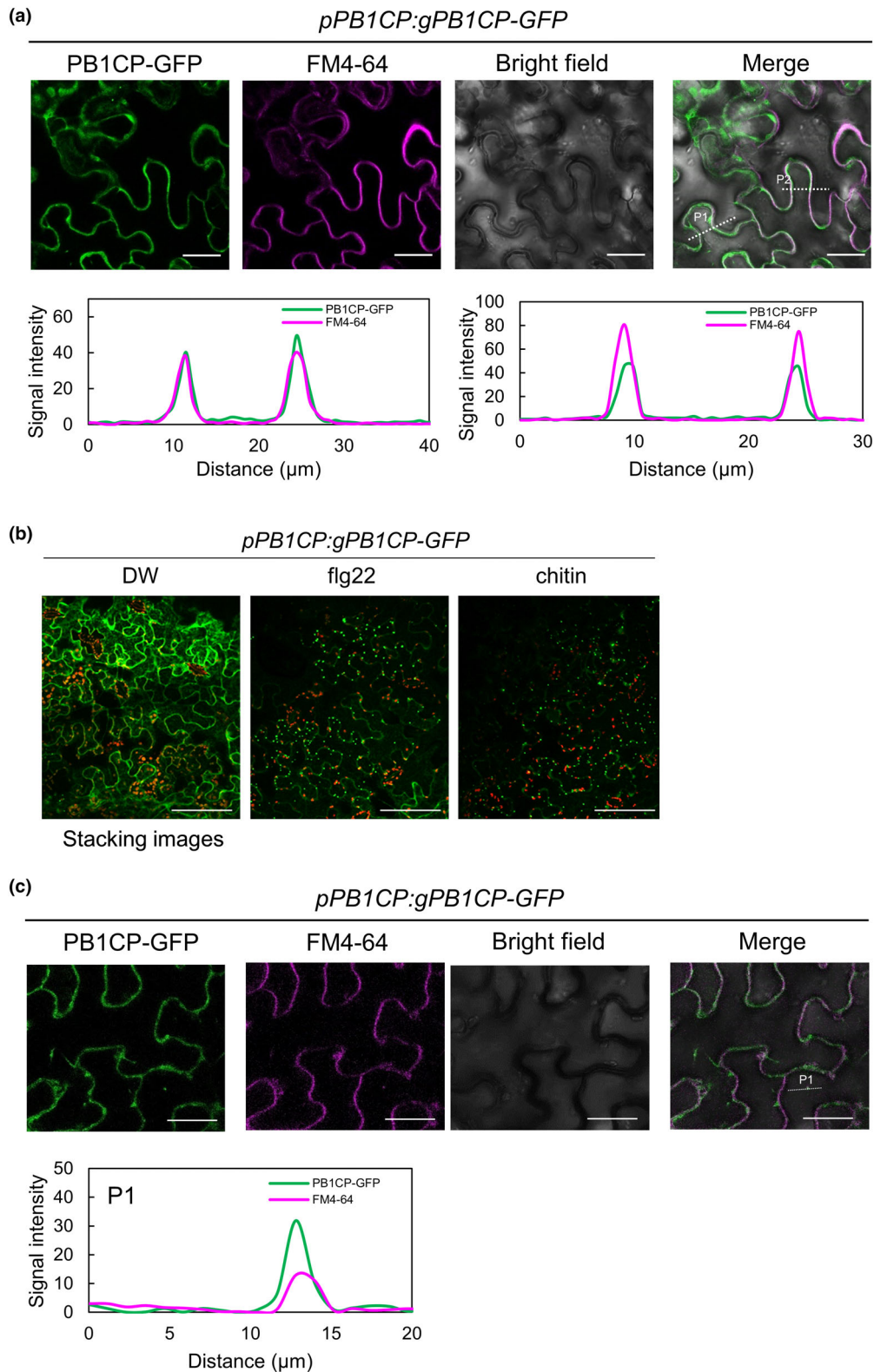
Fig. 6 PB1CP localizes at the cell periphery and pathogen-associated molecular pattern (PAMP) treatment induces the relocalization of PB1CP to small endomembrane compartments. (a) Subcellular localization of PB1CP-GFP expressed under its native promoter in *Nicotiana benthamiana*, and co-localization of PB1CP-GFP and FM4-64 signals at the plasma membrane. Fluorescence intensities of PB1CP-GFP were quantified at 500–540 nm and FM4-64 at 558–734 nm. Transections used for fluorescence intensity measurements are indicated by the white dashed lines (P1 and P2). The histograms show PB1CP-GFP and FM4-64 fluorescent intensities depicted by green and magenta lines, respectively. Bars, 30 μm. (b) The treatment with flg22 or chitin induced the formation of PB1CP signal foci. PB1CP-GFP was expressed in *N. benthamiana* under the control of its native promoter. Leaf disks were treated with DW, 10 μM flg22, or 100 μM chitin ((GlcNAc)$_7$) for 3 h. Bars, 100 μm. (c) Co-localization of PB1CP-GFP and FM4-64 signals in small endomembrane compartments after treatment with 10 μM flg22 for 3 h in *N. benthamiana*. Transections used for fluorescence intensity measurements are indicated by the white dashed line (P1). Bars, 30 μm. All the experiments were repeated three times with similar results.

moves from the plasma membrane to small endomembrane compartments in response to PAMPs.

Flg22 treatment induces the translocation of RBOHD with PB1CP to small endomembrane compartments

The observed translocation of PB1CP from the plasma membrane to small endomembrane compartments upon flg22 treatment suggests a potential role for PB1CP in facilitating the translocation of RBOHD to these specific compartments. To investigate the potential role of PB1CP in the translocation of RBOHD, we expressed CFP-RBOHD under the control of CaMV 35S promoter in *N. benthamiana*. The functionality of CFP-RBOHD was confirmed by observing its enhanced flg22-induced ROS production (Fig. S10a,b). Confocal microscopy analyses showed that CFP-RBOHD was localized at the plasma membrane, which was further confirmed by plasmolysis (Fig. S10c,d). To get a more precise observation of CFP-RBOHD protein dynamics, we used cycloheximide (CHX) to inhibit *de novo* synthesis of RBOHD because the supply of newly synthesized RBOHD to the plasma membrane could interfere with the accurate assessment of RBOHD dynamics. CHX treatment allowed us to focus on the pre-existing pool of RBOHD and gain better insights into its localization and behavior, especially after PAMP treatment. We co-expressed CFP-RBOHD and PB1CP-GFP in *N. benthamiana* and treated them with or without flg22 in the presence of CHX. CHX treatment resulted in a reduction in the overall intensity of CFP-RBOHD. However, the majority of CFP-RBOHD still exhibited clear localization at the plasma membrane (Fig. 7a). Interestingly, we occasionally observed small foci of CFP-RBOHD signal around the cell periphery and within the cytoplasm. Importantly, some of these CFP-RBOHD foci exhibited co-localization with FM4-64 and/or PB1CP-GFP (Fig. 7a). These results show the presence of CFP-RBOHD in endomembrane compartments with PB1-GFP. The co-localization of CFP-RBOHD foci with FM4-64 and PB1CP-GFP further supports the notion that PB1CP may play a role in the translocation of RBOHD from the plasma membrane to small endomembrane compartments.

Previous studies have demonstrated that flg22 treatment for a short duration (30–90 minutes) inhibits the endocytosis of RBOHD (Menzel *et al.*, 2019; Lee *et al.*, 2022). Consistent with these findings, we did not observe immediate changes in the localization of CFP-RBOHD following flg22 treatment for several hours. However, when we extended the treatment to 5 h, we found the number of small CFP-RBOHD signal foci significantly increased after flg22 (Fig. 7a). We quantified the number of small foci positive for FM4-64, as well as the number of FM4-64-stained small foci that co-localized with PB1CP-GFP, CFP-RBOHD, or both PB1CP-GFP and CFP-RBOHD (Fig. S11). After 5 h of flg22 treatment, there was a significant increase in the number of FM4-64-stained small foci that co-localized with PB1CP-GFP, CFP-RBOHD, or both PB1CP-GFP and CFP-RBOHD, while the total number of FM4-64-stained small foci remained unchanged (Fig. S11). The proportion of FM4-64-stained small foci containing both PB1CP-GFP and CFP-RBOHD increased from 1.5% to 30.5% of the total FM4-64-stained small foci. Additionally, the proportion of FM4-64-stained small foci containing only PB1CP-GFP increased from 6.5% to 20.8%, while the proportion of foci containing only CFP-RBOHD increased from 0.7% to 6.9%. These results show that the translocation of RBOHD is induced after long-time exposure to flg22 and that the majority of RBOHD-associated endomembrane compartments contain PB1CP. This suggests a potential involvement of PB1CP in endocytosis and degradation of RBOHD in the vacuole. To test this possibility, the seedlings of *pb1cp-2* mutant and *p35S:PB1CP-3xHA* line were treated with or without flg22 for 5 h and RBOHD protein levels were checked by immunoblotting (Fig. 8). In Col-0 seedlings, flg22 treatment led to the accumulation of RBOHD protein. However, in the *p35S:PB1CP-3xHA* line, both the basal abundance of RBOHD and the flg22-induced RBOHD accumulation were suppressed. These results suggest that PB1CP may be involved in the endocytosis and degradation of RBOHD. Unexpectedly, in the *pb1cp-2* mutant, the protein level of RBOHD remained unchanged (Fig. S4).

Discussion

Plants must tightly regulate the activity of RBOHs to minimize the potentially harmful effects of ROS, but the precise regulatory mechanisms of RBOH activity remain unknown. In our study, we identified PB1CP as a previously unknown binding protein to RBOHD and demonstrated its negative regulation of RBOHD upon PAMP perception through phenotypic characterization of *pb1cp* mutants and *p35S:PB1CP-3xHA* lines (Figs 2a–c, 3a–c). Our biochemical and microscopic analyses revealed potential regulatory mechanisms of RBOHD by PB1CP, including the removal of phosphorylated BIK1 from RBOHD and the promotion of RBOHD endocytosis.

PB1CP may negatively regulate RBOHD activity by disrupting BIK1 interaction

While CD of PB1CP weakly and stably associates with ND of RBOHD, the interaction becomes more pronounced upon PAMP treatment (Fig. 5a,b). The flg22-induced interaction of PB1CP to RBOHD leads to the release of phosphorylated BIK1 from RBOHD (Fig. 5d). These findings suggest a sequential regulation of RBOHD, where BIK1-mediated activation is followed by PB1CP-mediated downregulation. There are several possible
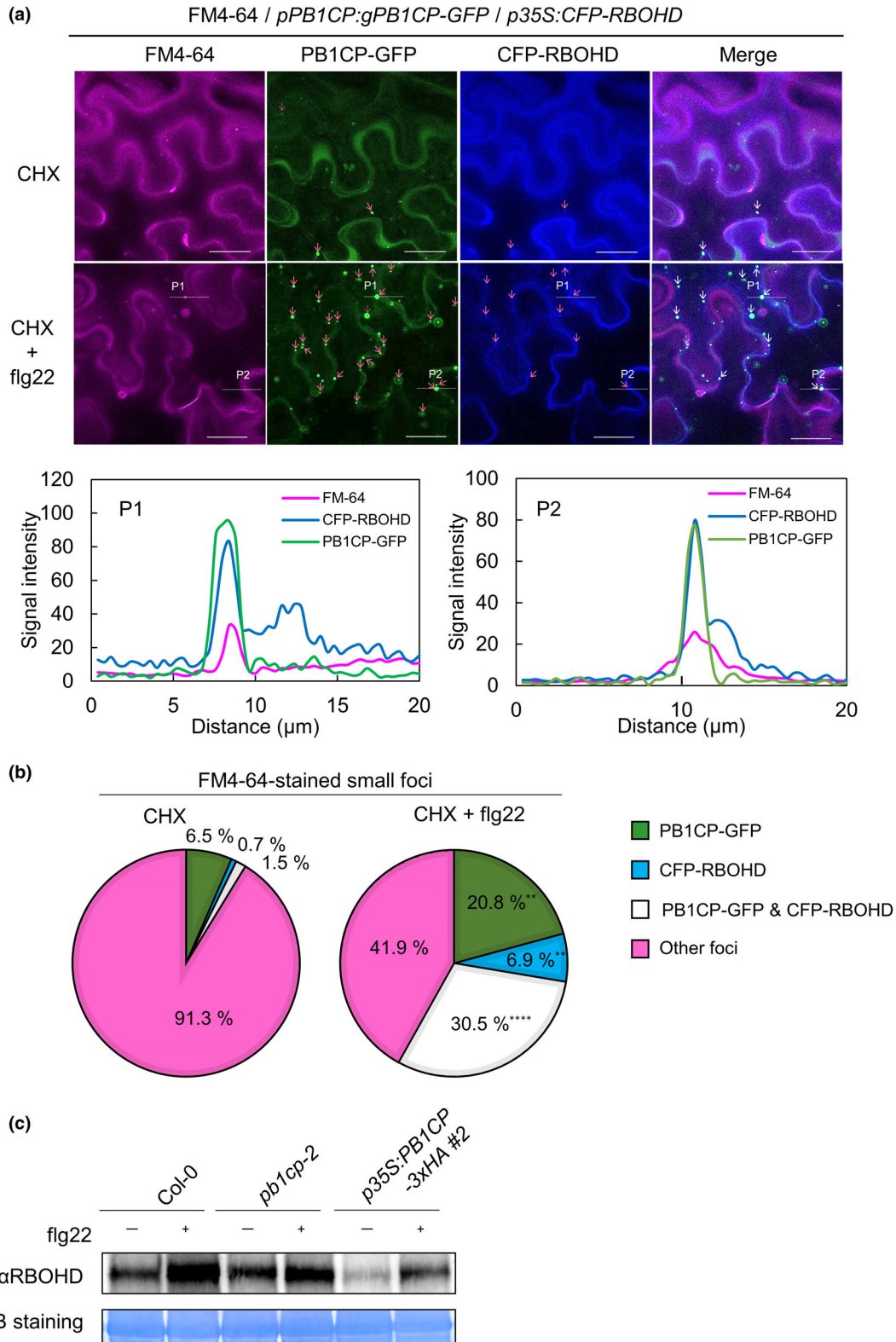
Fig. 7 Flg22 treatment induces the relocalization of RESPIRATORY BURST OXIDASE HOMOLOG D (RBOHD) from the plasma membrane to small endomembrane compartments with PB1CP. (a) Localization of PB1CP-GFP (*pPB1CP:gPB1CP-GFP*), CFP-RBOHD (*p35S:CFP-RBOHD*) and FM-4-64 in *Nicotiana benthamiana* after treatment with or without 10 μM flg22 for 5 h in the presence of 300 μM CHX. The fluorescence of PB1CP-GFP was measured at 510–550 nm, CFP-RBOHD at 440–477 nm, and FM4-64 at 580–630 nm to reduce potential fluorescence bleed-through. Co-localization of PB1CP-GFP or CFP-RBOHD with FM4-64 was indicated by magenta arrows, while co-localization of both PB1CP-GFP and CFP-RBOHD with FM4-64 was indicated by white arrows. Transections used for fluorescence intensity measurements are indicated by broken white lines (P1 and P2). The histograms show fluorescent intensities of PB1CP-GFP depicted by green lines, CFP-RBOHHD by blue lines and FM4-64 by magenta lines. Bars, 20 μm. (b) The percentage of FM4-64-stained small foci containing PB1CP-GFP, CFP-RBOHD, or both PB1CP-GFP and CFP-RBOHD in the total number of FM4-64-stained small foci. Numbers of the foci were counted in the 30 images (9685 μm^2 x 30) of the leaves treated with or without flg22. Asterisks indicate significant differences in the number of foci in the leaves treated with or without flg22 ($n = 30$, see Supporting Information Fig. S11; Student's *t*-test, **, $P \leq 0.01$; ****, $P \leq 0.001$). (c) Immunoblots of RBOHD protein in *pb1cp-2* mutant and *p35S:PB1CP-3xHA#2* line. Ten-day-old Arabidopsis seedlings were treated with or without 10 μM flg22 for 5 h, and RBOHD protein was detected with α-RBOHD antibody. The equal loading of protein samples was shown by CBB staining. The experiments were repeated three times with similar results.

mechanisms underlying this regulation. One possibility is that PB1CP binds with greater affinity to a phosphorylated surface of RBOHD facilitated by BIK1 or CPKs, compared with the non-phosphorylated form. Alternatively, upon phosphorylation by BIK1, CPKs, CRK2, or SIK1, or upon interaction with Ca^{2+}, RBOHD may undergo conformational changes, potentially exposing the buried PB1CP binding site. Another potential mechanism is that PB1CP might specifically bind to the homodimeric form of RBOHD, which is induced by PAMP treatment (Oda *et al.*, 2010). In either case, PB1CP likely competes with phosphorylated BIK1 for binding to RBOHD upon its activation by PAMPs, thereby contributing to the termination of the first phase of flg22-inducible ROS production (Fig. S12).

PB1CP might induce the endocytosis of RBOHD

Previous studies have demonstrated the cooperative regulation of RBOHD dynamics by clathrin- and microdomain-dependent endocytic pathways (Hao *et al.*, 2014). In our study, we have also identified clathrin-related components such as HAP13 and AP4M, as well as flg22-inducible components of detergent-resistant membranes including remorin and SPFH proteins, through co-immunoprecipitation with RBOHD (Table S1). These findings support the hypothesis that PB1CP-mediated relocalization of RBOHD involves endocytosis, and the observed small signal foci of CFP-RBOHD and PB1CP-GFP may represent endosomes. However, we cannot exclude the possibility that PB1CP-mediated relocalization of RBOHD also involves autophagy, as it has been shown to lead to the degradation of ubiquitinated plasma membrane proteins in vacuoles (Rodriguez-Furlan *et al.*, 2019).

Interestingly, even without PAMP treatment, we observed a limited number of endomembrane compartments containing both PB1CP-GFP and CFP-RBOHD. However, flg22 treatment significantly increased the number of PB1CP-associated endomembrane compartments. Importantly, the majority of RBOHD-associated endomembrane compartments contain PB1CP, suggesting PB1CP's potential involvement in the relocalization of RBOHD from the plasma membrane to endomembrane compartments. Note that PAL OF QUIRKY (POQ) which shares similarities with PB1CP (Fig. S4), binds to STRUBBELIG (SUB), a cell surface LRR-RK known to undergo *in vivo* ubiquitination and clathrin-mediated endocytosis (Trehin

et al., 2013; Gao *et al.*, 2019). While it remains uncertain whether POQ is involved in the endocytosis of SUB, a comparative analysis of the functions of PB1CP and POQ during endocytosis would be valuable in future studies.

Despite the clear evidence of RBOHD relocalization with PB1CP in the *N. benthamiana* system, we faced challenges in obtaining Arabidopsis transgenic lines expressing sufficient levels of fluorescence-tagged RBOHD under the native promoter for the microscopic analysis in our experimental setup, as reported by other research groups (Lee *et al.*, 2022). Even when using the *N. benthamiana* system, the expression of fluorescence-tagged RBOHD under its native promoter did not yield a robust signal for clear visualization of RBOHD relocalization into the small endomembrane compartments. Moreover, we observed instability in RBOHD protein levels in overexpressors driven by the 35S promoter in subsequent generations. These circumstances made it difficult to directly analyze the subcellular localization of RBOHD in *pb1cp* mutants or *p35S:PB1CP-3xHA* lines using microscopy-based approaches. However, we observed that overexpression of *PB1CP* leads to a reduction in the basal abundance of RBOHD and suppresses its flg22-induced accumulation in Arabidopsis, supporting the possible role of PB1CP in RBOHD relocalization and degradation. Notably, even in the absence of PAMP treatment, we observed a limited number of endomembrane compartments containing both PB1CP and RBOHD, implying that certain RBOHD molecules undergo endocytosis and subsequent degradation in the vacuole under basal conditions. The overexpression of PB1CP may enhance this process, leading to a reduction in RBOHD levels even before PAMP stimulation. Moreover, the overexpression of *PB1CP* might enhance PAMP-induced PB1CP-mediated RBOHD endocytosis, resulting in the suppression of PAMP-induced RBOHD accumulation.

However, in *pb1cp-2*, the accumulation of RBOHD was not detected, potentially due to the functional redundancy of PB1CP homologs (Fig. S4). Another possibility is that PB1CP selectively targets activated RBOHD molecules within the FLS2 complex upon flg22 treatment, facilitating their relocation to small endomembrane compartments. Nonactivated RBOHD molecules within other complexes may remain unaffected, explaining the limited observable accumulation of RBOHD in the *pb1cp-2* mutant. This contrasts with FLS2 endocytosis, where a significant portion of the FLS2 protein was shown to translocate to

endosomes when treated with high concentration of flg22 (10 μM) to activate majority of FLS2 in the cells (Robatzek *et al.*, 2006).

We also noted the translocation of PB1CP and RBOHD is a relatively slow response and is not visible several hours after flg22 treatment. This observation is consistent with previous studies that have shown a reduction in RBOHD endocytosis and an enhancement of RBOHD-mediated ROS production upon short-term flg22 treatment (Menzel *et al.*, 2019; Lee *et al.*, 2022). The translocation of PB1CP and RBOHD becomes apparent 3–5 h after flg22 treatment, coinciding with the attenuation of the second phase of flg22-inducible ROS production. This finding suggests that the suppression of RBOHD endocytosis during the initial stages of flg22 treatment may contribute to the upregulation of the first phase of ROS production, while PB1CP-mediated RBOHD endocytosis during the later stages of flg22 treatment may play a role in suppressing the second phase of ROS production (Fig. S12).

PB1CP-induced endocytosis might help reducing the amount of activated RBOHD

Our study suggests that PB1CP plays a negative regulatory role in two phases of ROS production induced by flg22 or elf18 (Figs 2, 3). This regulation is potentially achieved through the rapid removal of phosphorylated BIK1 from RBOHD and the gradual induction of RBOHD translocation (Fig. S12). By effectively shutting down both phases of ROS production, PB1CP may minimize the toxic effects of ROS on the plants. In this context, PB1CP's significance lies more in facilitating the recovery process after ROS-based immunity, allowing the plants to return to a healthy condition, rather than being involved in initiating a controlled ROS burst in response to pathogens. The PAMP-inducible interaction of PB1CP with RBOHD strongly suggests that PB1CP is responsible for deactivating the activated RBOHD, rather than suppressing its initial activation.

Potential roles of PB1 domain for the function of PB1CP

Although we found CD of PB1CP directly binds RBOHD and competes for interaction with BIK1 (Fig. 5b), the precise role of the N-terminal PB1 domain in PB1CP function is still unclear and requires further investigation. One possibility is that the PB1 domain of PB1CP induces multimerization, a critical step in protein aggregate formation, triggering the induction of autophagy. Notably, a well-characterized selective autophagy cargo receptor p62 also possesses a PB1 domain at its N-terminus and an ubiquitin-associated domain at the C-terminus, playing critical roles in multimerization and binding of polyubiquitinated cargo proteins, respectively (Chen *et al.*, 2021). Following the formation of aggregates containing p62 and cargo proteins, p62 recruits ATG8 through its AIM (Atg8-family interacting motif) sequence (W/Y/FxxL/I/V) to facilitate the formation of autophagosomes. It is tempting to speculate that PB1CP might function as an autophagy cargo receptor for RBOHD, utilizing its PB1 domain-mediated multimerization and PAMP-inducible

interaction with RBOHD through its C-terminus. It is also noteworthy that both PB1CP and RBOHD feature multiple AIM sequences, further pointing to the potential significance of this interaction in autophagy regulation. Nevertheless, comprehensive investigations are required to elucidate the precise mechanistic underpinnings of PB1CP's involvement in autophagy and its interplay with RBOHD.

Another possibility is that the PB1 domain of PB1CP induces heterodimerization with an unidentified regulator of RBOHD, as is the case for $p40^{phox}$ and $p67^{phox}$. One potential candidate is a member of the 'kinase-derived PB1 family'. Yeast two-hybrid analysis has indeed shown that PB1CP interacts with AT3G48240, another member of the 'kinase-derived PB1 family' (Arabidopsis Interactome Mapping Consortium, 2011). However, the specific role of AT3G48240 in the regulation of RBOHD, if any, still needs to be demonstrated.

Another potential interactor is a member of the PB1 domain-containing 'kinase domain family' (Fig. S4). Similar to the role of PBL13, these kinases might have the ability to phosphorylate the CD of RBOHD, particularly at residue T912, resulting in enhanced ubiquitination of RBOHD and decreased protein abundance. Additionally, these kinases could potentially phosphorylate and activate PIRE, a protein that triggers the ubiquitination of RBOHD and facilitates its endocytosis (Lin *et al.*, 2015; Lee *et al.*, 2020). Therefore, it would be worth investigating the molecular relationship between PB1CP and PIRE in the context of RBOHD endocytosis.

Final remarks

Our study uncovers novel mechanisms involved in the downregulation of RBOHD-mediated ROS production, highlighting the roles of PB1CP in removing the key activator BIK1 from RBOHD and promoting RBOHD translocation. Further investigations are required to precisely determine the nature of the endomembrane compartments containing RBOHD and PB1CP to clarify molecular mechanisms underlying PB1CP's regulation of RBOHD by identifying the specific interactor of PB1CP through its PB1 domain and obtaining stronger evidence regarding the role of PB1CP in RBOHD relocalization. Additionally, it would be interesting to explore whether PB1CP-based regulation extends to other plant RBOHs, considering their diverse functions in stress adaptation, growth, and development. These future directions will provide a deeper understanding of the broader regulatory network governing ROS signaling in plants.

Competing interests

None declared.

Author contributions

YK performed co-immunoprecipitation of RBOHD in Arabidopsis and *N. benthamiana*. JS, PD and FLHM performed LC–MS/MS analyses. NM helped to generate constructs for transient expression of RBOHD-associated proteins in *N. benthamiana*. YG and YK performed immunoblotting and ROS assays. YG performed the other experiments. YK, CZ and KS supervised the research. YK and YG wrote the draft manuscript. All of the authors read, commented on, and approved the manuscript.

ORCID

Paul Derbyshire https://orcid.org/0000-0002-5095-9397
Yukihisa Goto https://orcid.org/0000-0003-3616-320X
Yasuhiro Kadota https://orcid.org/0000-0002-4782-1418
Noriko Maki https://orcid.org/0000-0002-8750-7685
Frank L. H. Menke https://orcid.org/0000-0003-2490-4824
Ken Shirasu https://orcid.org/0000-0002-0349-3870
Jan Sklenar https://orcid.org/0000-0003-1858-2574
Cyril Zipfel https://orcid.org/0000-0003-4935-8583

Data availability

The data that support the findings of this study are available in the Supporting Information of this article.

References

Arabidopsis Interactome Mapping Consortium. 2011. Evidence for network evolution in an Arabidopsis interactome map. *Science* **333**: 601–607.

Asai S, Ohta K, Yoshioka H. 2008. MAPK signaling regulates nitric oxide and NADPH oxidase-dependent oxidative bursts in *Nicotiana benthamiana*. *Plant Cell* **20**: 1390–1406.

Bedard K, Krause KH. 2007. The NOX family of ROS-generating NADPH oxidases: physiology and pathophysiology. *Physiological Reviews* **87**: 245–313.

Canton J, Grinstein S. 2014. Priming and activation of NADPH oxidases in plants and animals. *Trends in Immunology* **35**: 405–407.

Chen W, Shen T, Wang L, Lu K. 2021. Oligomerization of selective autophagy receptors for the targeting and degradation of protein aggregates. *Cell* **10**: 1989.

Chinchilla D, Zipfel C, Robatzek S, Kemmerling B, Nurnberger T, Jones JD, Felix G, Boller T. 2007. A flagellin-induced complex of the receptor FLS2 and BAK1 initiates plant defence. *Nature* **448**: 497–500.

Dubiella U, Seybold H, Durian G, Komander E, Lassig R, Witte CP, Schulze WX, Romeis T. 2013. Calcium-dependent protein kinase/NADPH oxidase activation circuit is required for rapid defense signal propagation. *Proceedings of the National Academy of Sciences, USA* **110**: 8744–8749.

Entila F, Han X, Mine A, Schulze-Lefert P, Tsuda K. 2023. Commensal lifestyle regulated by a negative feedback loop between Arabidopsis ROS and the bacterial T2SS. *bioRxiv*. doi: 10.1101/2023.05.09.539802.

Frei Dit Frey N, Mbengue M, Kwaaitaal M, Nitsch L, Altenbach D, Haweker H, Lozano-Duran R, Njo MF, Beeckman T, Huettel B et al. 2012. Plasma membrane calcium ATPases are important components of receptor-mediated signaling in plant immune responses and development. *Plant Physiology* **159**: 798–809.

Gao J, Chaudhary A, Vaddepalli P, Nagel MK, Isono E, Schneitz K. 2019. The Arabidopsis receptor kinase STRUBBELIG undergoes clathrin-dependent endocytosis. *Journal of Experimental Botany* **70**: 3881–3894.

Gao X, Chen X, Lin W, Chen S, Lu D, Niu Y, Li L, Cheng C, McCormack M, Sheen J et al. 2013. Bifurcation of Arabidopsis NLR immune signaling via Ca^{2+}-dependent protein kinases. *PLoS Pathogens* **9**: e1003127.

George J, Stegmann M, Monaghan J, Bailey-Serres J, Zipfel C. 2023. Arabidopsis translation initiation factor binding protein CBE1 negatively regulates accumulation of the NADPH oxidase RESPIRATORY BURST OXIDASE HOMOLOG D. *Journal of Biological Chemistry* **7**: 105018.

Goto Y, Maki N, Ichihashi Y, Kitazawa D, Igarashi D, Kadota Y, Shirasu K. 2020. Exogenous treatment with glutamate induces immune responses in *Arabidopsis*. *Molecular Plant–Microbe Interactions* **33**: 474–487.

Groemping Y, Rittinger K. 2005. Activation and assembly of the NADPH oxidase: a structural perspective. *Biochemical Journal* **386**: 401–416.

Hao H, Fan L, Chen T, Li R, Li X, He Q, Botella MA, Lin J. 2014. Clathrin and membrane microdomains cooperatively regulate RbohD dynamics and activity in *Arabidopsis*. *Plant Cell* **26**: 1729–1745.

Hiruma K, Saijo Y. 2016. Plant inoculation with the fungal leaf pathogen *Colletotrichum higginsianum*. *Methods in Molecular Biology* **1398**: 313–318.

Kadota Y, Liebrand TWH, Goto Y, Sklenar J, Derbyshire P, Menke FLH, Torres MA, Molina A, Zipfel C, Coaker G et al. 2019. Quantitative phosphoproteomic analysis reveals common regulatory mechanisms between effector- and PAMP-triggered immunity in plants. *New Phytologist* **221**: 2160–2175.

Kadota Y, Macho AP, Zipfel C. 2016. Immunoprecipitation of plasma membrane receptor-like kinases for identification of phosphorylation sites and associated proteins. *Methods in Molecular Biology* **1363**: 133–144.

Kadota Y, Shirasu K, Zipfel C. 2015. Regulation of the NADPH oxidase RBOHD during plant immunity. *Plant and Cell Physiology* **56**: 1472–1480.

Kadota Y, Sklenar J, Derbyshire P, Stransfeld L, Asai S, Ntoukakis V, Jones JD, Shirasu K, Menke F, Jones A et al. 2014. Direct regulation of the NADPH oxidase RBOHD by the PRR-associated kinase BIK1 during plant immunity. *Molecular Cell* **54**: 43–55.

Kimura S, Hunter K, Vaahtera L, Tran HC, Citterico M, Vaattovaara A, Rokka A, Stolze SC, Harzen A, Meissner L et al. 2020. CRK2 and C-terminal phosphorylation of NADPH oxidase RBOHD regulate reactive oxygen species production in Arabidopsis. *Plant Cell* **32**: 1063–1080.

Kobayashi M, Ohura I, Kawakita K, Yokota N, Fujiwara M, Shimamoto K, Doke N, Yoshioka H. 2007. Calcium-dependent protein kinases regulate the production of reactive oxygen species by potato NADPH oxidase. *Plant Cell* **19**: 1065–1080.

Lambeth JD, Cheng G, Arnold RS, Edens WA. 2000. Novel homologs of gp91phox. *Trends in Biochemical Sciences* **25**: 459–461.

Lee D, Lal NK, Lin ZD, Ma S, Liu J, Castro B, Toruno T, Dinesh-Kumar SP, Coaker G. 2020. Regulation of reactive oxygen species during plant immunity through phosphorylation and ubiquitination of RBOHD. *Nature Communications* **11**: 1838.

Lee J, Nguyen HH, Park Y, Lin J, Hwang I. 2022. Spatial regulation of RBOHD via AtECA4-mediated recycling and clathrin-mediated endocytosis contributes to ROS accumulation during salt stress response but not flg22-induced immune response. *The Plant Journal* **109**: 816–830.

Lewis JD, Abada W, Ma W, Guttman DS, Desveaux D. 2008. The HopZ family of *Pseudomonas syringae* type III effectors require myristoylation for virulence and avirulence functions in *Arabidopsis thaliana*. *Journal of Bacteriology* **190**: 2880–2891.

Li L, Li M, Yu L, Zhou Z, Liang X, Liu Z, Cai G, Gao L, Zhang X, Wang Y et al. 2014. The FLS2-associated kinase BIK1 directly phosphorylates the NADPH oxidase RbohD to control plant immunity. *Cell Host & Microbe* **15**: 329–338.

Li X, Zhang H, Tian L, Huang L, Liu S, Li D, Song F. 2015. Tomato SlRbohB, a member of the NADPH oxidase family, is required for disease resistance against *Botrytis cinerea* and tolerance to drought stress. *Frontiers in Plant Science* **6**: 463.

Liang X, Ding P, Lian K, Wang J, Ma M, Li L, Li L, Li M, Zhang X, Chen S et al. 2016. Arabidopsis heterotrimeric G proteins regulate immunity by directly coupling to the FLS2 receptor. *eLife* **5**: e13568.

Lin ZJ, Liebrand TW, Yadeta KA, Coaker G. 2015. PBL13 is a serine/threonine protein kinase that negatively regulates Arabidopsis immune responses. *Plant Physiology* **169**: 2950–2962.

Liu Z, Wu Y, Yang F, Zhang Y, Chen S, Xie Q, Tian X, Zhou JM. 2013. BIK1 interacts with PEPRs to mediate ethylene-induced immunity. *Proceedings of the National Academy of Sciences, USA* **110**: 6205–6210.

Lu D, Wu S, Gao X, Zhang Y, Shan L, He P. 2010. A receptor-like cytoplasmic kinase, BIK1, associates with a flagellin receptor complex to initiate plant innate immunity. *Proceedings of the National Academy of Sciences, USA* **107**: 496–501.

Luna E, Pastor V, Robert J, Flors V, Mauch-Mani B, Ton J. 2011. Callose deposition: a multifaceted plant defense response. *Molecular Plant–Microbe Interactions* **24**: 183–193.

Marino D, Dunand C, Puppo A, Pauly N. 2012. A burst of plant NADPH oxidases. *Trends in Plant Science* **17**: 9–15.

Mbengue M, Bourdais G, Gervasi F, Beck M, Zhou J, Spallek T, Bartels S, Boller T, Ueda T, Kuhn H et al. 2016. Clathrin-dependent endocytosis is required for immunity mediated by pattern recognition receptor kinases. *Proceedings of the National Academy of Sciences, USA* **113**: 11034–11039.

Melotto M, Underwood WA, He SY. 2008. Role of stomata in plant innate immunity and foliar bacterial diseases. *Annual Review of Phytopathology* **46**: 101–122.

Menzel W, Stenzel I, Helbig LM, Krishnamoorthy P, Neumann S, Eschen-Lippold L, Mareike Heilmann M, Lee J, Heilmann I. 2019. A PAMP-triggered MAPK cascade inhibits phosphatidylinositol 4,5-bisphosphate production by PIP5K6 in *Arabidopsis thaliana*. *New Phytologist* **224**: 833–847.

Mersmann S, Bourdais G, Rietz S, Robatzek S. 2010. Ethylene signaling regulates accumulation of the FLS2 receptor and is required for the oxidative burst contributing to plant immunity. *Plant Physiology* **154**: 391–400.

Miya A, Albert P, Shinya T, Desaki Y, Ichimura K, Shirasu K, Narusaka Y, Kawakami N, Kaku H, Shibuya N. 2007. CERK1, a LysM receptor kinase, is essential for chitin elicitor signaling in Arabidopsis. *Proceedings of the National Academy of Sciences, USA* **104**: 19613–19618.

Moeder W, Yoshioka K. 2008. Lesion mimic mutants. *Plant Signaling & Behavior* **3**: 764–767.

Morales J, Kadota Y, Zipfel C, Molina A, Torres MA. 2016. The Arabidopsis NADPH oxidases RbohD and RbohF display differential expression patterns and contributions during plant immunity. *Journal of Experimental Botany* **67**: 1663–1676.

Müller S, Kursula I, Zou P, Wilmanns M. 2006. Crystal structure of the PB1 domain of NBR1. *FEBS Letters* **580**: 341–344.

Mutte SK, Weijers D. 2020. Deep evolutionary history of the Phox and Bem1 (PB1) domain across Eukaryotes. *Scientific Reports* **10**: 3797.

Narusaka M, Shiraishi T, Iwabuchi M, Narusaka Y. 2010. Monitoring fungal viability and development in plants infected with *Colletotrichum higginsianum* by quantitative reverse transcription-polymerase chain reaction. *Journal of General Plant Pathology* **76**: 1–6.

O'Connell RJ, Thon MR, Hacquard S, Amyotte SG, Kleemann J, Torres MF, Damm U, Buiate EA, Epstein L, Alkan N et al. 2012. Lifestyle transitions in plant pathogenic *Colletotrichum* fungi deciphered by genome and transcriptome analyses. *Nature Genetics* **44**: 1060–1065.

Oda T, Hashimoto H, Kuwabara N, Akashi S, Hayashi K, Kojima C, Wong HL, Kawasaki T, Shimamoto K, Sato M et al. 2010. Structure of the N-terminal regulatory domain of a plant NADPH oxidase and its functional implications. *Journal of Biological Chemistry* **285**: 1435–1445.

Ogasawara Y, Kaya H, Hiraoka G, Yumoto F, Kimura S, Kadota Y, Hishinuma H, Senzaki E, Yamagoe S, Nagata K et al. 2008. Synergistic activation of the Arabidopsis NADPH oxidase AtrbohD by Ca^{2+} and phosphorylation. *Journal of Biological Chemistry* **283**: 8885–8892.

Pfeilmeier S, Petti GC, Bortfeld-Miller M, Daniel B, Field CM, Sunagawa S, Vorholt JA. 2021. The plant NADPH oxidase RBOHD is required for microbiota homeostasis in leaves. *Nature Microbiology* **6**: 852–864.

Pfeilmeier S, Werz A, Ote M, Bortfeld-Miller M, Kirner P, Keppler A, Hemmerle L, Gäbelein CG, Pestalozzi CM, Vorholt JA. 2023. Dysbiosis of a leaf microbiome is caused by enzyme secretion of opportunistic *Xanthomonas* strains. *bioRxiv*. doi: 10.1101/2023.05.09.539948.

Robatzek S, Chinchilla D, Boller T. 2006. Ligand-induced endocytosis of the pattern recognition receptor FLS2 in Arabidopsis. *Genes & Development* **20**: 537–542.

Rodriguez-Furlan C, Minina EA, Hicks GR. 2019. Remove, recycle, degrade: regulating plasma membrane protein accumulation. *Plant Cell* **31**: 2833–2854.

Roux M, Schwessinger B, Albrecht C, Chinchilla D, Jones A, Holton N, Malinovsky FG, Tor M, De Vries S, Zipfel C. 2011. The Arabidopsis leucine-rich repeat receptor-like kinases BAK1/SERK3 and BKK1/SERK4 are required for innate immunity to hemibiotrophic and biotrophic pathogens. *Plant Cell* **23**: 2440–2455.

Schindelin J, Arganda-Carreras I, Frise E, Kaynig V, Longair M, Pietzsch T, Preibisch S, Rueden C, Saalfeld S, Schmid B et al. 2012. Fiji: an open-source platform for biological-image analysis. *Nature Methods* **9**: 676–682.

Segal AW. 2016. NADPH oxidases as electrochemical generators to produce ion fluxes and turgor in fungi, plants and humans. *Open Biology* **6**: 160028.

Shinya T, Yamaguchi K, Desaki Y, Yamada K, Narisawa T, Kobayashi Y, Maeda K, Suzuki M, Tanimoto T, Takeda J et al. 2014. Selective regulation of thechitin-induced defense response by the Arabidopsis receptor-like cytoplasmic kinase PBL27. *The Plant Journal* **79**: 56–66.

Stegmann M, Monaghan J, Smakowska-Luzan E, Rovenich H, Lehner A, Holton N, Belkhadir Y, Zipfel C. 2017. The receptor kinase FER is a RALF-regulated scaffold controlling plant immune signaling. *Science* **355**: 287–289.

Sumimoto H. 2008. Structure, regulation and evolution of Nox-family NADPH oxidases that produce reactive oxygen species. *FEBS Journal* **275**: 3249–3277.

Sun Y, Li L, Macho AP, Han Z, Hu Z, Zipfel C, Zhou JM, Chai J. 2013. Structural basis for flg22-induced activation of the Arabidopsis FLS2-BAK1 immune complex. *Science* **342**: 624–628.

Suzuki N, Miller G, Salazar C, Mondal HA, Shulaev E, Cortes DF, Shuman JL, Luo X, Shah J, Schlauch K et al. 2013. Temporal-spatial interaction between reactive oxygen species and abscisic acid regulates rapid systemic acclimation in plants. *Plant Cell* **25**: 3553–3569.

Thor K, Jiang S, Michard E, George J, Scherzer S, Huang S, Dindas J, Derbyshire P, Leitao N, Defalco TA et al. 2020. The calcium-permeable channel OSCA1.3 regulates plant stomatal immunity. *Nature* **585**: 569–573.

Tian W, Hou C, Ren Z, Wang C, Zhao F, Dahlbeck D, Hu S, Zhang L, Niu Q, Li L et al. 2019. A calmodulin-gated calcium channel links pathogen patterns to plant immunity. *Nature* **572**: 131–135.

Torres MA, Dangl JL. 2005. Functions of the respiratory burst oxidase in biotic interactions, abiotic stress and development. *Current Opinion in Plant Biology* **8**: 397–403.

Torres MA, Dangl JL, Jones JD. 2002. Arabidopsis gp91phox homologues AtrbohD and AtrbohF are required for accumulation of reactive oxygen intermediates in the plant defense response. *Proceedings of the National Academy of Sciences, USA* **99**: 517–522.

Trehin C, Schrempp S, Chauvet A, Berne-Dedieu A, Thierry AM, Faure JE, Negrutiu I, Morel P. 2013. QUIRKY interacts with STRUBBELIG and PAL OF QUIRKY to regulate cell growth anisotropy during Arabidopsis gynoecium development. *Development* **140**: 4807–4817.

Wong HL, Pinontoan R, Hayashi K, Tabata R, Yaeno T, Hasegawa K, Kojima C, Yoshioka H, Iba K, Kawasaki T et al. 2007. Regulation of rice NADPH oxidase by binding of Rac GTPase to its N-terminal extension. *Plant Cell* **19**: 4022–4034.

Wu Y, Xun Q, Guo Y, Zhang J, Cheng K, Shi T, He K, Hou S, Gou X, Li J. 2016. Genome-wide expression pattern analyses of the Arabidopsis leucine-rich repeat receptor-like kinases. *Molecular Plant* **9**: 289–300.

Yeh YH, Panzeri D, Kadota Y, Huang YC, Huang PY, Tao CN, Roux M, Chien HC, Chin TC, Chu PW et al. 2016. The Arabidopsis malectin-like/LRR-RLK IOS1 is critical for BAK1-dependent and BAK1-independent pattern-triggered immunity. *Plant Cell* **28**: 1701–1721.

Yuan M, Jiang Z, Bi G, Nomura K, Liu M, Wang Y, Cai B, Zhou JM, He SY, Xin XF. 2021. Pattern-recognition receptors are required for NLR-mediated plant immunity. *Nature* **592**: 105–109.

Yun BW, Feechan A, Yin M, Saidi NB, Le Bihan T, Yu M, Moore JW, Kang JG, Kwon E, Spoel SH et al. 2011. S-nitrosylation of NADPH oxidase regulates cell death in plant immunity. *Nature* **478**: 264–268.

Zhang J, Li W, Xiang T, Liu Z, Laluk K, Ding X, Zou Y, Gao M, Zhang X, Chen S et al. 2010. Receptor-like cytoplasmic kinases integrate signaling from

multiple plant immune receptors and are targeted by a *Pseudomonas* syringae effector. *Cell Host & Microbe* 7: 290–301.

Zhang M, Chiang YH, Toruño TY, Lee D, Ma M, Liang X, Lal NK, Lemos M, Lu YJ, Ma S et al. 2018. The MAP4 Kinase SIK1 ensures robust extracellular ROS burst and antibacterial immunity in plants. *Cell Host & Microbe* 24: 379–391.

Supporting Information

Additional Supporting Information may be found online in the Supporting Information section at the end of the article.

Fig. S1 Co-immunoprecipitation of 3xFLAG-RESPIRATORY BURST OXIDASE HOMOLOG D (RBOHD) to identify RBOHD-associated proteins.

Fig. S2 Rapid functional analyses of RESPIRATORY BURST OXIDASE HOMOLOG D-associated proteins on flg22-induced reactive oxygen species production in *Nicotiana benthamiana*.

Fig. S3 PB1CP inhibits flg22-induced reactive oxygen species production in *Nicotiana benthamiana*.

Fig. S4 Phylogenetic tree of full-length proteins belonging to 'kinase-derived PB1 family' and 'kinase-containing PB1 family' groups in Arabidopsis.

Fig. S5 T-DNA insertion and expression in *pb1cp* mutants.

Fig. S6 Expression of *PB1CP-3xHA* in *p35S:PB1CP-3xHA* lines.

Fig. S7 elf18 and chitin, but not flg22, weakly induce the accumulation of *PB1CP* transcript.

Fig. S8 PB1CP does not affect the transcript level of *PB1CP*.

Fig. S9 *pb1cp* mutants and *p35S:PB1CP-3xHA* lines do not show defects in resistance against bacteria.

Fig. S10 CFP-RESPIRATORY BURST OXIDASE HOMOLOG D is functional and localized at the plasma membrane in *Nicotiana benthamiana*.

Fig. S11 flg22 Treatment increased the number of FM4-64-stained small foci containing PB1CP-GFP, CFP-RESPIRATORY BURST OXIDASE HOMOLOG D (RBOHD), or both PB1CP-GFP and CFP-RBOHD. *CFP-RBOHD* or *PB1CP-GFP* were co-expressed in *Nicotiana benthamiana* by Agroinfiltration.

Fig. S12 Model for PAMP-induced RESPIRATORY BURST OXIDASE HOMOLOG D (RBOHD) activation and PB1CP-mediated RBOHD downregulation during PTI.

Methods S1 Additional methods not included in the main text.

Table S1 List of RESPIRATORY BURST OXIDASE HOMOLOG D-associated proteins.

Table S2 Summary of the effect of RESPIRATORY BURST OXIDASE HOMOLOG D-associated proteins on flg22-induced reactive oxygen species production in *Nicotiana benthamiana* and primers used in this work.

Video S1 PB1CP-GFP signals move around the cell periphery and in the cytoplasm.

Video S2 PB1CP-GFP signals in the cell periphery and cytoplasm were reduced, and PB1CP-GFP signal foci appeared in those regions.

Please note: Wiley is not responsible for the content or functionality of any Supporting Information supplied by the authors. Any queries (other than missing material) should be directed to the *New Phytologist* Central Office.